Accepted in
Applied Soft computing
http://dx.doi.org/10.1016/j.asoc.2007.07.003

Flank Wear Prediction in Drilling using Back Propagation Neural Network and Radial Basis Function Network

S. S. Panda[1], # D. Chakraborty[1], S. K. Pal[2]
[1]*Department of Mechanical Engineering, Indian Institute of Technology, Guwahti Assam-781039, India, sspanda@iitg.ernet.in*
[2] *Department of mechanical Engineering, Indian Institute of technology Kharagpur WB-721302, India, skpal@mech.iitkgp.ernet.in*

Abstract
In the present work, two different types of artificial neural network (ANN) architectures viz. back propagation neural network (BPNN) and radial basis function network (RBFN) have been used in an attempt to predict flank wear in drills. Flank wear in drill depends upon speed, feed rate, drill diameter and hence these parameters along with other derived parameters such as thrust force, torque and vibration have been used to predict flank wear using ANN. Effect of using increasing number of sensors in the efficacy of predicting drill wear by using ANN has been studied. It has been observed that inclusion of vibration signal along with thrust force and torque leads to better prediction of drill wear. The results obtained from the two different ANN architectures have been compared and some useful conclusions have been made.

Keywords: *Neuron, Cluster, Center vector, Euclidian distance, Sensor signal, Flank wear*

Corresponding author. Tel No.: +91-361-2582666; fax: +91-361-2690762
E-mail address: chakra@iitg.ernet.in

1 Introduction

Manufacturing industries are trying to reduce the operation cost as well as better quality of product. So automation with online monitoring in metal cutting operation is a new approach toward improvement of the quality of the product as well as reduction of the overall cost of the product. Monitoring of drill wear is an important issue since wear on drill affect the hole quality and tool life of the drill. Direct visual inspection of cutting edge is not feasible and hence indirect methods using sensory feed back during machining has been is use to assess the wear of the drill.

For improving the performance of decision-making in tool condition monitoring, different type of intelligent systems has been put forwarded by many authors. Following paragraph describes some of the relevant researches in this direction.

Lin and Ting [1] used the neural network model to study the drill wear and observed that the training error in case of sample mode converges faster than that in case of batch mode. Li and Tso [2] monitored the tool wear based on current signals of spindle motor and feed motor using regression model. Tsao [3] used the radial basis function network (RBFN) and adaptive based radial basis function network (ARBFN) to predict the flank wear, and compared their results with experimental observation. Abbu [4] predicted wear rate in drilling using Fast Fourier Transformation (FFT) of vibration signature as an input to ANN. Multiple objectives linear programming models for optimizing drill hole quality with different cutting conditions such as speed and feed rate was proposed by Kim and Ramulu [5]. A.K Singh *et al.* [6] used back propagation neural network for prediction of flank wear of High Speed Steel (HSS) drill in a copper work piece using spindle speed, feed rate, drill diameter, thrust force and torque as input parameters and maximum flank wear as output parameter in a neural network. S.S Panda *et al.* [7] used back propagation neural network for prediction of flank wear of HSS drill in a mild steel work piece using the spindle speed, feed rate, drill diameter, thrust force, torque and chip thickness as input parameters and maximum flank wear as output parameter to neural network and concluded that inclusion of chip thickness as an input parameter to network leads to better prediction of flank wear. Li *et al.* [8] proposed hybrid learning for monitoring of drill wear using a combination of fuzzy system and neural network. Kuo and Kohen [9] applied a modified fuzzy neural network for detecting the defective sensor signal using membership function at the input node and fuzzy rule base. Lo [10] described the tool state in turning operation using artificial neuro fuzzy inference system (ANFIS) architecture, and concluded that higher accuracy could be achieved in the case of triangular and bell shape membership function. Hashmi *et al.* [11] proposed a fuzzy model for correlating the drilling speed with hardness of work material. They have used triangular membership function with fuzzy rule base in there analysis. Chung-Chen Tsao [12] used radial basis function network to forecast the flank wear of different coated drill using hybrid learning rule i.e combination of least square method and gradient descent method. G.H Lim [13] in his work correlated the flank wear of tool with the acceleration amplitude of

vibration signature in turning operation and he concluded that vibration acceleration produces two-peak amplitudes just before tool failure. Marek Balazinski *et al.* [14] used three artificial intelligence (AI) methods: feed forward back propagation neural network, fuzzy decisions support system and an artificial neural network based fuzzy inference system to monitor the flank wear in turning operation. Toshiyuki Obikawa *et al.* [15] used unsupervised and self-organizing neural network Adaptive Resonance Theory (ART2) for monitoring of flank wear in high speed machining operation. C. Chungchoo *et al.* [16] used fuzzy neural network model for online tool wear estimation in CNC turning. D.K Sonar *et al.* [17] used radial basis function neural network for predicting the surface roughness in turning operation

The present paper aims at studying the efficacy of ANN in predicting drill wear when trained with different combination of sensor signals. Comparison has also been made between standard BPNN model and RBFN in predicting drill wear on cast iron work-piece.

2. Back propagation neural network

2.1 Back propagation neural network architecture

Back propagation neural network is a three-layered feed forward architecture. The three layers are input layer, hidden layer and output layer. Functioning of back propagation proceeds in three stages, namely learning or training, testing or inferences and validation.

Fig. 1 shows the *l*-*m*-*n* (*l* input neurons, *m* hidden neurons, and *n* output neurons) architecture of a back propagation neural network model. Input layer receives information from the external sources and passes this information to the network for processing. Hidden layer receives information from the input layer, and does all the information processing, and output layer receives processed information from the network, and sends the results out to an external receptor. The input signals are modified by interconnection weight, known as weight factor w_{ji}, which represents the interconnection of i^{th} node of the first layer to j^{th} node of the second layer. The sum of modified signals (total activation) is then modified by a sigmoidal transfer function. Similarly, outputs signal of hidden layer are modified by interconnection weight (w_{kj}) of k^{th} node of output layer to j^{th} node of hidden layer. The sum of the modified signal is then modified by sigmoidal transfer function and output is collected at output layer.

Let $I_p = (I_{p1}, I_{p2}, ...I_{pl}), p = 1, 2....N$ be the p^{th} pattern among N input patterns. Where. W_{ji} and W_{kj} are connection weights between i^{th} input neuron to j^{th} hidden neuron, and j^{th} hidden neuron to k^{th} output neuron, respectively.

Output from a neuron in the input layer is,

$$O_{pi} = I_{pi}, i = 1, 2.....l \qquad (1)$$

Output from a neuron in the hidden layer is,

$$O_{pj} = f(NET_{pj}) = f\left(\sum_{i=0}^{l} W_{ji} O_{pi}\right), j = 1, 2.....m \qquad (2)$$

Output from a neuron in the output layer is,

$$O_{pk} = f(NET_{pk}) = f\left(\sum_{j=0}^{m} W_{kj} O_{pj}\right), k = 1, 2.....n \qquad (3)$$

2.2 Learning or training in back propagation neural network

Batch mode type of supervised learning has been used in the present case, where, interconnection weights are adjusted using delta rule algorithm after sending the entire training sample to the network. During training, the predicted output is compared with the desired output, and the mean square error is calculated. If the mean square error is more than a prescribed limiting value, it is back propagated from output to input, and weights are further modified till the error or number of iterations is within a prescribed limit.

Mean square error, E_p for pattern p is defined as

$$E_p = \sum_{i=1}^{n} \frac{1}{2} (D_{pi} - O_{pi})^2 \qquad (4)$$

where, D_{pi} is the target output, and O_{pi} is the computed output for the i^{th} pattern.

Weight change at any time t, is given by

$$\Delta W(t) = -\eta E_p(t) + \alpha \times \Delta W(t-1) \qquad (5)$$

where, η is learning rate, and α momentum parameter.

2.3 Testing and validation of back propagation neural network

Entire experimental data set is divided into training set, testing set and validation set. The error on the testing set is monitored during the training process. The testing error will normally

decrease during the initial phase of training, as does the training set error. However, when the network begins to over fit the data, the error on the testing set will typically begin to rise. When the testing error starts increasing for a specified number of iterations, the training is stopped; and the weights and biases at the minimum value of the testing error are returned. The unseen data (validation set) is then fed to the trained network to check the percentage variation of predicted output (flank wear) in comparison to the actual wear.

3 Radial basis function network

3.1 Architecture of radial basis function network

Basically radial basis function network is composed of large number of simple and highly interconnected artificial neurons and can be organized into several layer, i.e input layer, hidden layer, and output layer [18] as shown in Fig. 2.

Input layer:

An input pattern enters the input layer and is subjected to direct transfer function and output from input layer is same as input pattern. Number of nodes in the input layer is equal to the dimension of input vector L.

Output from input layer with element $I_{i(i=1\,to\,L)}$ is I_i.

Hidden layer:

The hidden layer does all the important process and these nodes satisfy a unique property being radially symmetry. Being *radially symmetry* it must have the following

a. *A center vector* v_j in the input space, made up of cluster center with element $v_{ji(j=1\,to\,M)}$.' $M \le P$' where M is the number of center vectors and P is number of training patterns. The vector typically is stored as weight factors from input layer to hidden layer.

b. *A distance measure* to determine how far an input pattern with element I_i is from cluster center v_{ji}. We have used Euclidean distance norm for this purpose.

   Euclidean distance $ed_j = \left\| I - v_j \right\| = \sqrt{\sum_{i=1}^{L} (I_i - v_{ji})^2}$ (6)

c. *A transfer function* which transfers Euclidean distance to give output for each node. In our case we used the gaussian function for this purpose.

$$output_j = \exp(ed_j^{\,2} \div \sigma^2) \quad (7)$$

where σ is the spread parameter determined from

$$\sigma = \max(ed)/\sqrt{M} \quad (8)$$

and $\max(ed)$ is maximum Euclidean distance between selected centers and M is the number of centers.

Output layer:

There are weight factor $w_{kj(k=1\,to\,N,\,j=1\,to\,M)}$ between k^{th} nodes of output layer and j^{th} nodes of hidden layer.' N 'is the dimension of output vector. Output from output layer transferred through a transfer function like log sigmoid or tan sigmoid.

Output from the output layer is given by

$$output_k = f(\sum_{k=1}^{N} w_{kj} \times output_j) \quad (9)$$

3.2 Training of radial basis function network

In the present case training based on self-organized selection of centers has been considered as described in the following section.

3.2.1 Self-Organized selection of centers

1. It is a self-organizing network known as '**SOM**' in which initial centers vector v_j was chosen randomly. The only restriction is that these initial values must be different.
2. Training samples are read and Euclidean distance was calculated for the initial center vector as per eq^n (6)
3. The corresponding center vector was modified closest to the training sample as

$$\begin{aligned} &v_j^{new} = v_j^{old} + \eta \times (I_{pi} - v_j^{old}) \\ &P = training\ sample \\ &j = no\ of\ \ centre\ vector \\ &i = input\ node \\ &\eta = learning\ rate\ i.e\ 0 < \alpha < 1 \end{aligned} \quad (10)$$

4. This process was continued for fixed number of iteration until no noticeable change was observed for the center vector v_j . This is known as ***k-means clustering*** algorithm [18], a special case of competitive (winners takes all) learning process.
5. Spread parameter was calculated as per eq^n (8)
6. Weights of output layer are initialized to small random values, and output from output layer was calculated as per eq^n (9).
7. Mean square error (MSE) of training sample was calculated. If the MSE training does not reach the goal specified then weight is updated based on gradient descent method. The weight was updated in the present case in batch mode.
8. The process was carried out for a definite number of iteration.

4 Experimental Set-up

In the present work, a radial drilling machine (Batliboi Limited, BR618 model) is used for the drilling operation. High-speed steel (HSS) drills with different diameters have been used for drilling in cast iron work piece at different cutting conditions. Different sensory devices such as dynamometer, vibration analyzer are used for conducting the experiments as shown in Fig. 3. High-speed steel (HSS) drill of four different diameters (chemical composition and geometrical specification are listed in Tables 1 (a) and (b)) have been used to drill holes on cast iron (refer Tables 2 (a) and (b) for specification and compositions) specimen at different cutting conditions. In all the drilling operations performed in the present work, no coolant has been used. Root mean square (RMS*)* values of thrust force and torque signal are recorded through a piezo-electric dynamometer (Kistler, 9272). Signals from the dynamometer were passed through low pass filter, amplified through charge amplifier (Kistler, type 5015 model), and stored in the computer through a data acquisition system (Advantech, PCL 818 HG, 100 KHz span length). Two numbers of piezo electric accelerometer has been used to capture vibration signals. One accelerometer has been attached on the top surface of the cast iron specimen to extract feed vibration and other on the side surface of the cast iron specimen to extract radial vibration. Signals from accelerometer were passed through vibration analyzer (Bruel & Kjaer, type 3560 D) in the frequency range 7 Hz-25.6 kHz. RMS of maximum amplitude of vibration both in feed and radial direction are collected through Bruel & Kjaer pulse software version 7 and is stored in

the computer through data acquisition system through data recorder type (Bruel & Kjaer, Type 7701) with sampling rate of 266.9 sample per second. 1.966 Mega sample are collected through data recorder type of span length of 25.6 kHz. The digital microscope along with Carl-Zeiss software interfacing has been used to measure flank wear. The maximum flank wear is used as the criterion to characterize the drill condition, and is obtained by measuring the wear at different points on either of the cutting edges. Photographs of gradual wear build-up process in the drill of 9 mm diameter for two different feed rates as observed under microscope are shown in Fig. 4(a)-4(b).

5 Results and Discussion

Drilling operations have been conducted over a wide a range of cutting condition. Spindle speed has been varied in the range 250 *rpm* to 500 *rpm* in four steps. Feed rate has been varied from 0.13 to 0.36 *mm/rev* in four steps. High-speed steel (HSS) drills of four different diameters of (9*mm*, 10*mm*, *11mm* and 12*mm*) have been used for drilling through holes of 15mm thickness in cast iron plates Different combinations of three design variables viz. spindle speed, feed rate and drill diameter have been used to perform 64 different drilling operations on cast iron plate. For each of these conditions, thrust force and torque have been measured using dynamometer and the data are stored in the computer. Similarly for each cutting condition, feed vibration and radial vibrations have been measured using accelerometer, and the data are stored in the computer through the LabView (Version7) software. Corresponding to each cutting condition, maximum flank wear has also been measured using digital microscope. The results of the experiment are tabulated in Table 3, which shows the thrust force, torque, amplitude of vibrations and the flank wear corresponding to 64 different cutting conditions.

5.1 Effect of important process parameters on sensor signal

Signals (thrust force, torque and vibration components) collected at different cutting conditions definitely have some dependence on the process parameters like (feed rate, drill diameter and spindle speed) as listed in Table 3. Hence effect of individual process parameter on sensor signals has been analyzed in the following section.

5.1.1 Effect of speed, feed rate and drill diameter on thrust force

Fig. 5 shows variation of thrust force with feed rate for different spindle speeds for a 9 mm diameter drill. It could be observed that thrust force increases with increase in feed rate for a given spindle speed and this is due to the already established facts that increase in feed rate increase the chip load action thus thrust force increases. It could also be observed that the increasing trend of thrust force with feed rate is more pronounced at lower range of spindle speeds (at 250rpm and 315rpm). Similarly it could be observed that thrust force decreases with increase in spindle speed and this is due to fact that increase in spindle speed increase the temperature generation during shearing action of cutting tool, and hence it soften the material of the work piece which results in the reduction of the thrust force.

Fig. 6 shows the variation of the thrust force with drill diameter at constant spindle speed of 500 rpm. It could be observed that thrust force increases with increase in drill diameter and this is due to facts that increase in drill diameter increases chip load action and thus thrust force increases. It can also be observed from Fig. 6 that thrust force is more sensitive to feed rate compared to drill diameter. This may be due to the fact that an increase in feed rate along the axial direction imparts more chip load than that due to of an increase in diameter along the circumferential direction.

5.1.2 Effect of speed, feed rate and drill diameter on torque

Fig. 7 shows variation of torque with feed rate for different spindle speeds for a 9 mm diameter drill. It could be observed that torque increases with increase in feed rate for a given spindle speed due to the same reason as explained in the case of thrust force.

Fig. 8 shows the variation of the torque with drill diameter at constant spindle speed of 500 rpm. It could be observed that torque increases with increase in drill diameter due to same reason as explained in case of thrust force.

5.1.3 Effect of speed, feed rate and drill diameter on vibration signal

Fig. 9 shows variation of feed vibration with feed rate for different spindle speeds for a 9 mm diameter drill. It could be observed that increase in feed rate reduces the vibration spectra, which may be due to fact that mass of the material, removed in terms of chip act as constraint, which prevents it (tool) to deflect from its location. Another reason may be with increase in feed rate, tool engagement with work piece increases and hence the stiffness of the whole system (tool-

work piece engagement) increases, thus deflection of the cutting tool along feed direction reduces. Similarly it could also be observed that feed vibration increases with increase in spindle speed and this is due to fact that increases in spindle speed (RPM) increases surface speed of drill thus centrifugal force increases which will try to deflect the end point of drill which acts as cantilever.

Fig. 10 shows the variation of the feed vibration with drill diameter at constant spindle speed of 500 rpm. It could be observed that feed vibration amplitude increases with increase in drill diameter and this is due to the fact that increase in drill diameter increases surface speed of drill thus increasing the centrifugal force which will deflect the end point of drill. Though increase in drill diameter increases stiffness of the system, leading to reduction in vibration spectra, but it is dominated by the surface speed of the drill and the combined effect lead to increase in vibration spectra.

Fig. 11 shows the variation of the both components of vibration spectra with spindle speed at constant feed rate of 0.13 mm/rev and constant drill diameter of 9 mm. It could be observed that radial vibration is more predominate than feed vibration which may be due to the fact that the drill acts as cantilever has sufficient freedom to move along radial direction rather then feed direction.

5.2 Wear prediction by back propagation neural network

Back propagation neural network architectures, prepared using various combination of input parameter such as spindle speed, feed rate, drill diameter, thrust force, torque, feed vibration, and radial vibration. Neural network architectures with and without vibration signals have been tried in an attempt to improve the efficacy of the network. In all the cases, the output of the network has been flank wear only.

Out of the 64 data sets, 37 data sets (training set) are selected at random and have been used for training the network and 17 data set (testing set) are used to evaluate the testing error to be used as stopping criteria for the network. The remaining 10 data set (validation set) are used to evaluate the validation error of the network. The normalized data sets are used for training the network. The data sets are normalized in the range of 0.1 to 0.9 using

$$y = 0.1 + 0.8\left(\frac{x - x_{\min}}{x_{\max} - x_{\min}}\right) \qquad (11)$$

where,

x = Actual value,

x_{max} = Maximum value of x,

x_{min} = Minimum value of x,

y = Normalized value corresponding to x.

Best network architecture (i.e., number of hidden layers, number of neurons in the hidden layers, learning rate and momentum coefficient) has been obtained by trial and error based on mean square error MSE in training, MSE in testing, and the number of iterations. Large number of runs were given for selecting the best architecture and table 4 shows only some of them along with the number of neuron in the hidden layer, MSE for training, MSE for testing, number of iteration and corresponding percentage of error while validating the sample.

5.2.1 Network architecture without vibration

In this case, the network has five input nodes corresponding to five input parameters (drill diameter, spindle speed, feed rate, thrust force and torque) and one output node corresponding to one output parameter (flank wear of drill). The optimum architecture has been attained by hit and trial after trying large number of different network architectures some of which has been shown in Table 4. Based on these observation the optimum network obtained in the present case is 5-7-1 with η=0.3 and α=0.9.

Fig. 12 shows the variation of MSE in training and testing with number of iterations for network of 5-7-1 with η=0.3 and α=0.9. It could be observed that network could be trained till 3495 iterations after which it starts over fitting and at this point MSE for testing as 0.000347 and MSE for training as 0.000221. After the network has been trained, it has been validated with unknown data sample. Fig. 13 shows percentage of error between actual value and the predicted value and it could be observed that the predicted values from the neural network are within $\pm 7.03\%$ of the actual values.

5.2.2 Network architecture with feed vibration

Next, attempt has been made in preparing network architecture considering an extra input node (feed vibration). In this case, the network has six input nodes corresponding to six input

parameters (drill diameter, spindle speed, feed rate, thrust force, torque and feed vibration) and one output node corresponding to one output parameter (flank wear of drill). The optimum architecture has been attained by hit and trial after trying large number of different network architecture, some of which are tabulated in Table 4. Based on these observation the optimum network obtained in the present case is 6-3-1 with η =0.3 and α =0.6

Fig. 14 shows the variation of mean square error in training and testing with number of iteration for network 6-3-1 with η =0.3 and α =0.6. It could be observed that network could be trained till 1991 iterations with MSE for testing as 0.000451 and MSE for training as 0.000673. After the network has been trained, it has been validated with unknown data sample. Fig. 15 shows percentage of error between actual value and the predicted value and it can be observed that the predicted values are within $\pm 6.25\%$ of the actual values.

5.2.3 Network architecture with both feed vibration and radial vibration

Here an attempt has been made in preparing network architecture considering both components of vibration spectra i.e feed vibration and radial vibration. In this case network has seven input nodes corresponding to seven input parameters (drill diameter, spindle speed, feed rate, thrust force, torque, feed vibration and radial vibration) and one output node corresponding to one output parameter (flank wear of drill). The optimum architecture has been attained by hit and trial after trying large number of different network architecture, some of these architectures corresponding to their number of neuron in hidden layer, mean square error of testing and number of iterations have been tabulated in Table 4. Based on these observation the optimum network obtained in the present case is 7-10-1 with η =0.6 and α =0.9.

Fig. 16 shows the variation of MSE in training and MSE in testing with number of iteration for network 7-10-1 with η =0.6 and α =0.9. It could be observed that network could be trained till 5404 iterations with MSE for testing as 0.000356 and MSE for training as 0.000201. After the network has been trained, it has been validated with unknown data samples. Fig. 17 shows percentage of error between actual value and the predicted value and it could be observed that the predicted values are within $\pm 6.17\%$.

5.3 Wear predictions by self-organizing network

In this section an attempt has been made in selecting the methodology of the network. As seen from back propagation neural network that increase in number of input node increases the accuracy of prediction. Hence in the present method all input parameters (drill diameter, spindle speed, feed rate, thrust force, torque, feed vibration and radial vibration) have been considered with one output parameter (flank wear). Network architectures, have been prepared using various combination of number of centre vector in hidden layer, learning rate η and momentum coefficient α .

Out of the 64 data set, the network has been trained in batch mode using randomly selected 45 data set and rest 19 data set are used to evaluate the testing error to be used as stopping criterion for the network. The data sets are normalized in the range of 0.1 to 0.9 using equation (11).

Best network architecture (i.e., number of centre vector in the hidden layers, learning rate and momentum coefficient) has been obtained by trial and error based on mean square error in training, testing, and the number of iterations. Large numbers of runs were given for selecting the best architecture and Table 5 shows some of them along with number of centre vectors, mean square error for training, mean square error for testing, and number of iteration and corresponding percentage of error of testing sample. Number of centre vectors varies from 10 to 40 in 4 steps and range of η and α varies from 0.1 to 0.9.

In this case, the network has seven input nodes and one output node. The optimum network architecture has been attained by hit and trial after trying large number of different network architectures. Some of these architectures corresponding to their number of centre vector, mean square error of testing and number of iterations have been tabulated in Table 5. Based on these observations, the optimum network obtained in the present case is 7-40-1 with $\eta = 0.3$ and $\alpha = 0.9$.

Fig. 18 shows the variation of mean square error in training and testing with number of iteration for network 7-40-1 with $\eta = 0.3$ and $\alpha = 0.9$. It could be observed that network has been trained till 435 iteration in which MSE for testing is 0.000393 and MSE for training is 0.001827. It can also be observed from the Fig. 18 that mean square error of training and testing sample rapidly reduces within 100 iterations and thereafter reduces slowly till the network over fits.

After the network has been trained, it has been verified with testing sample. Fig. 19 shows percentage of error between actual value and the predicted value and it can be observed that the present 7-40-1 self organizing network with $\eta = 0.3$ and $\alpha = 0.9$ predicts the result within $\pm 8.2\,\%$.

Fig. 20 shows variation of Euclidian distance with number of iterations for the optimum network of 7-40-1 with $\eta = 0.3$ and $\alpha = 0.9$. In the self organizing network, center vector which is farthest away from the clustered of training sample, is iteratively modified closest to training sample or in other words the stored weights between input and hidden layer are changed. It can be observed for a training sample that there was no noticeable change of center vector after about 200 iterations. So during simulation, a sufficient number of iteration of near by 200 has been given in order to achieve the stability of centre vector or input layer weights.

6 Conclusions

Process parameters such as drill diameter, spindle speed, feed are supplemented with sensors signals such as thrust force, torque and vibration signals for training a back propagation neural network as well as a radial basis function network for predicting flank wear in drill. It has been observed from the present study that both BPNN and RBFN can predict the drill flank wear reasonably well. From the present work, the following specific conclusions have been drawn.

1. Inclusion of vibration signals as input to train neural network results in a better-trained network, which can predict the wear with more accuracy.
2. BPNN can predict the wear more accurately compared to RBFN.
3. While the error in prediction is more in RBFN compared to that in the case of BPNN, RBFN can learn the pattern much faster compared to BPNN and could be used advantageously in on-line tool wear monitoring.

References

[1] S.C. Lin, C.J. Ting, “Drill wear monitoring using neural network”, International Journal of Machine Tool Manufacture, 36 (1996) 465-475.

[2] Li Xiaoli, S.K. Tso, “Drill wear monitoring based on current signals”, Journal Wear 231 (1999) 172-178.

[3] C.C. Tsao, “Prediction of flank wear of different coated drills for JIS SUS 304 stainless steel using neural network”, Journal of Material Processing Technology 123 (2002) 354-360.

[4] I. Abbu-Mahfouz, “Drilling wear detection and classification using vibration signals and artificial neural network”, International Journal of Machine Tool Manufacturer 43 (2003) 707-720.
[5] D. Kim, M. Ramulu, “Drilling process optimization for graphite/ bismaleimide-titanium alloy stack”, Journal of Composite structures 63 (2004) 101-114.
[6] A.K. Singh, S.S. Panda, S.K. Pal, D. Chakraborty, “Predicting drill wear using an artificial neural network”, International journal of advanced manufacturing technology DOI 10.1007/s00170-004-2376-0
[7] S.S Panada, A.K Singh, D. Chakraborty, S.K Pal, “Drill Wear Monitoring using Back Propagation Neural Network”, Journal of Material Processing Technology 172 (2006) 283–290.
[8] X. Li,S. Dong, P.K. Nenuvinod, “Hybrid learning for tool wear monitoring”, International journal of advanced manufacturing technology 16 (2000) 303-307.
[9] R.J. Kuo, P.H. Cohen, “Multi-sensor integration for online tool wear estimation through radial basis function networks and fuzzy neural network”, Neural network 12 (1999) 355-370.
[10] S.-P. Lo, “The application of an ANFIS and grey system method in turning tool-failure detection”, International journal of advanced manufacturing technology 19 (2002) 564-572.
[11] K. Hashmi, I.D. Graham, B. Mills, “Fuzzy logic based data selection for drilling process”, Journal of material processing technology 108 (2000) 55-61.
[12] Chung-Chen Tsao, “Prediction of flank wear of different coated drills for JIS SUS 304 stainless steel using neural network”, Journal of material processing technology 123 (2002) 354-360.
[13] G.H Lim, “Tool wear monitoring in machine turning”, Journal of material processing technology 51 (1995) 25-36.
[14] Marek Balazinski, Ernest Czogala, Krzysztof Jemielniak, Jacek Leski, “tool condition monitoring using artificial intelligence methods”, Engineering application of artificial intelligence 15 (2002) 73-80.
[15] Toshiyuki Obikawa, Jun Shinozuka, “Monitoring of flank wear of coated tools in high speed machining with neural network ART2”, International journal of machine tool manufacture 44 (2004) 1311-1318.
[16] C Chungchoo, D Saini, “on line tool wear estimation in CNC turning operation using fuzzy neural network model”, International journal of machine tool and manufacturer 42 (2002) 29-40.
[17] D.K Sonar, U.S Dixit, D.K Ojha, “The application of radial basis function neural network for predicting the surface roughness in a turning process”, International journal of advanced manufacturing technology DOI 10.1007/s00170-004-2258-5
[18] Simon Haykin, Neural network a comprehensive foundation, Prentice-Hall of India Pvt. Ltd., 2004

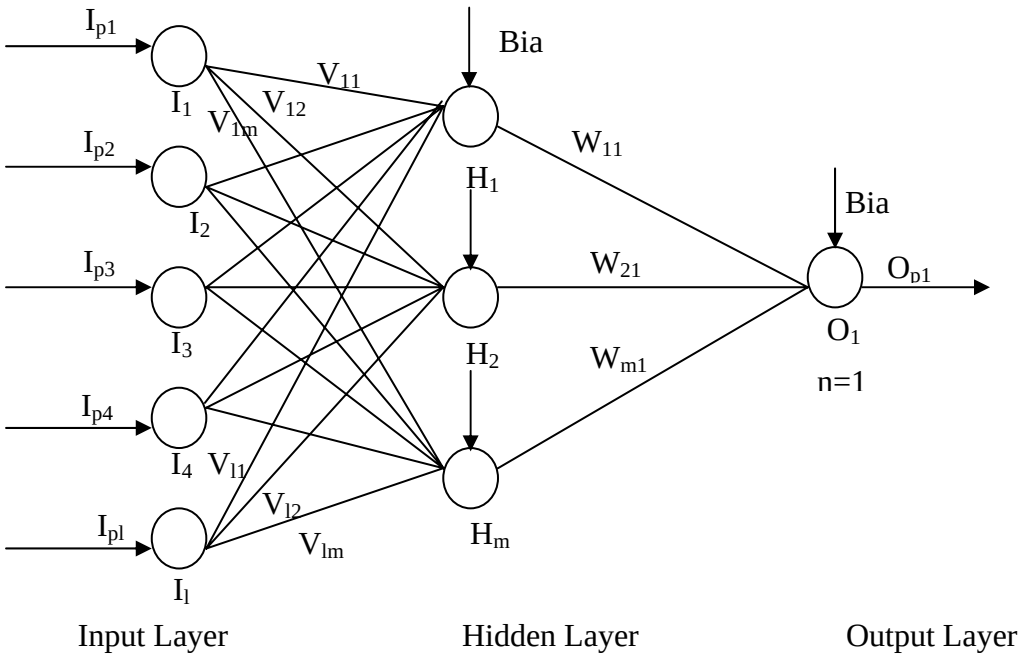

Fig. 1 Architecture of back propagation network

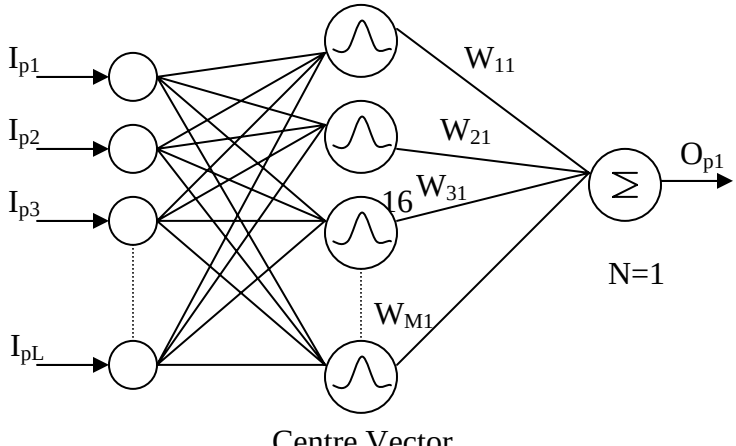

Fig. 2 Architecture of self organizing network

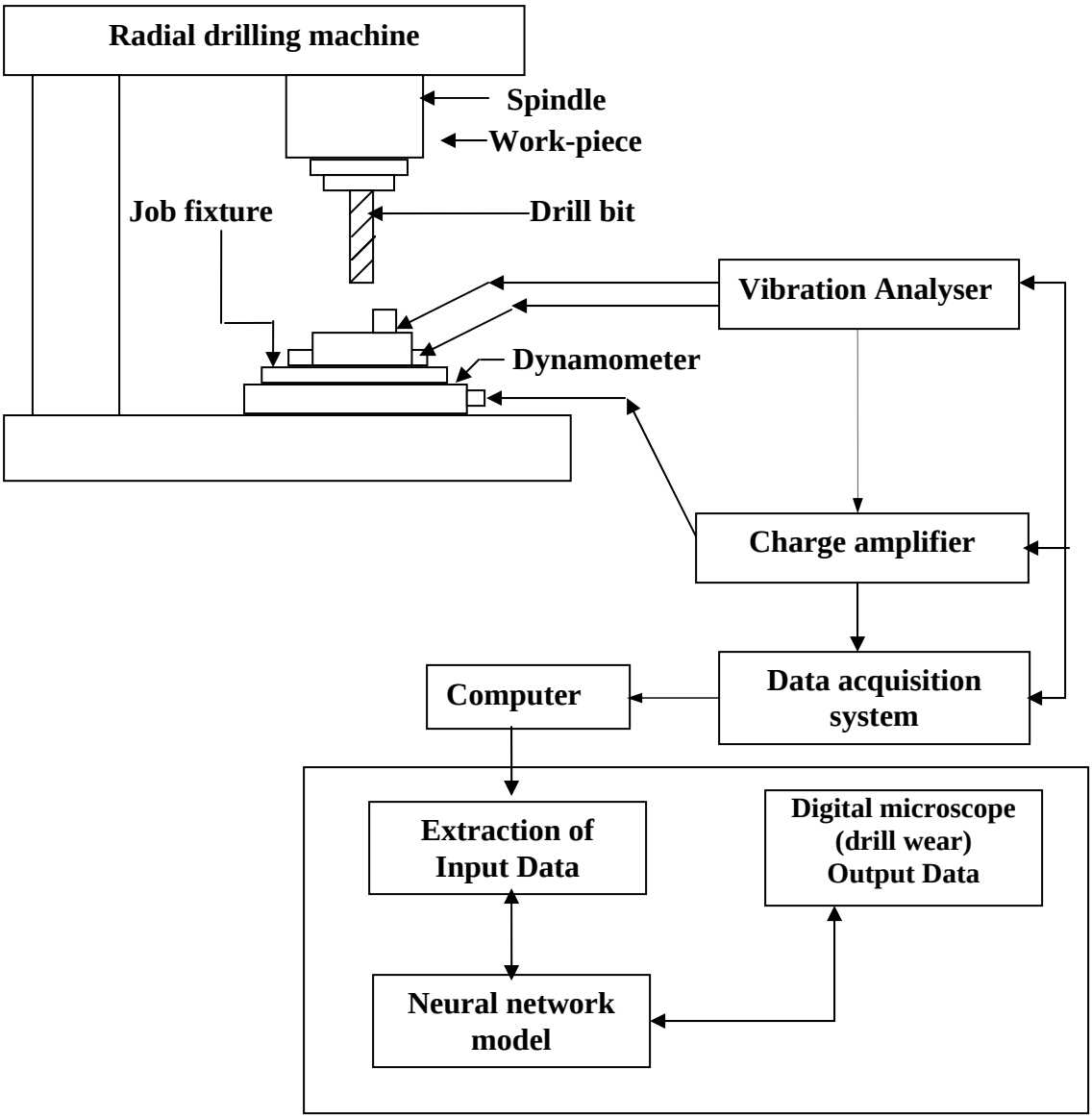

Fig. 3 Schematic diagram of the experimental set-up

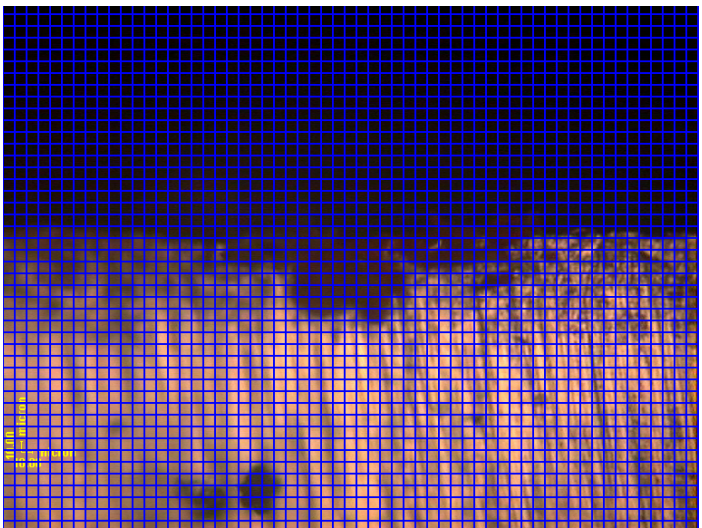

Fig. 4(a) Flank wear of 10 mm diameter at spindle speed 400 rpm and feed rate 0.13 mm/rev.

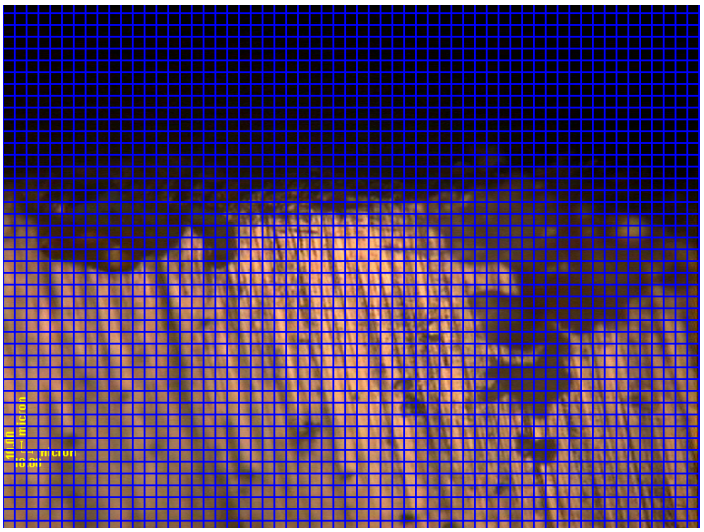

Fig. 4(b) Flank wear of 10 mm diameter at spindle speed 400 rpm and feed rate 0.36 mm/rev.

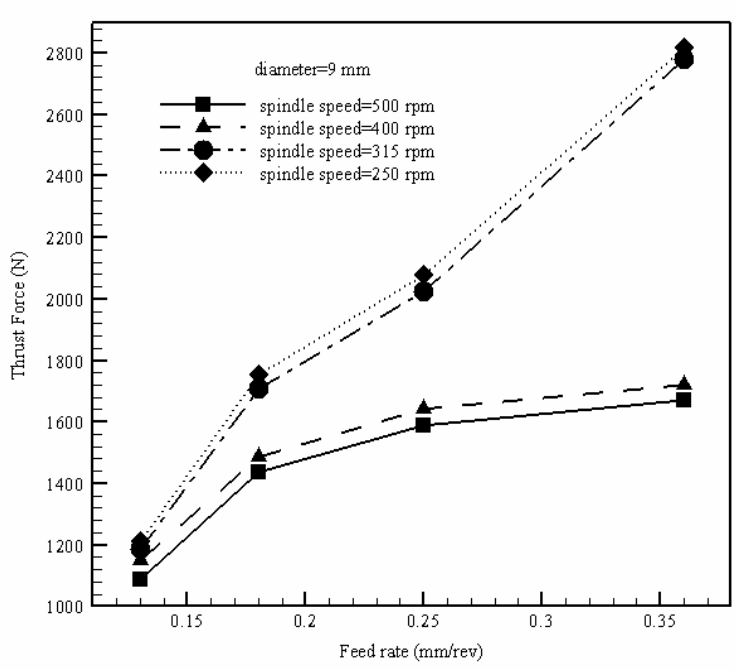

Fig. 5 Effect of feed rate on thrust force

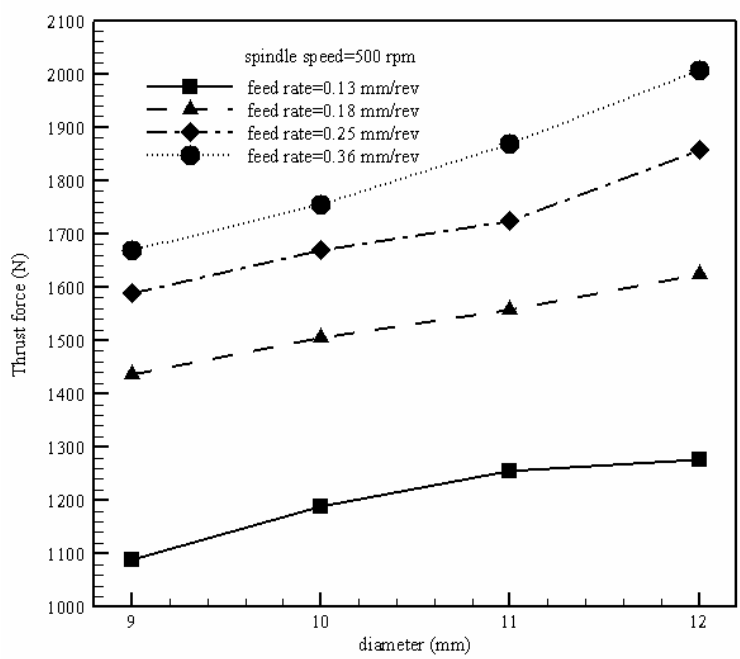

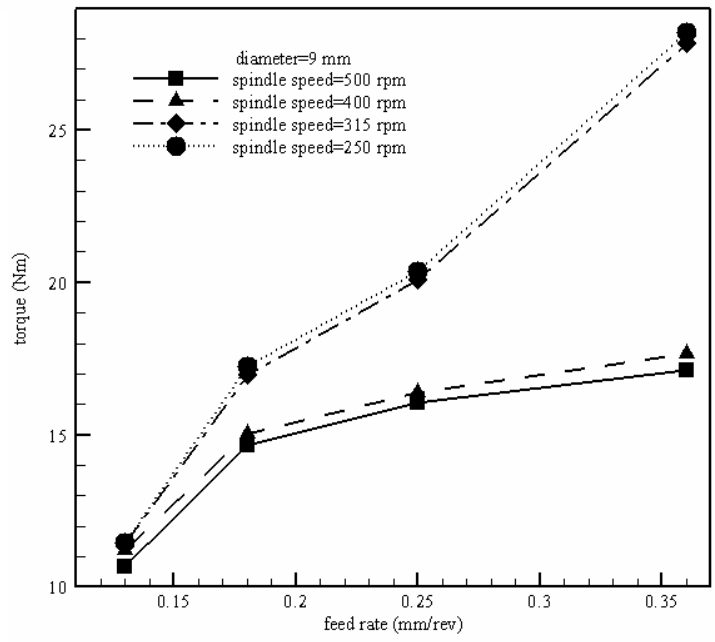

Fig. 6 Effect of drill diameter on thrust force

Fig. 7 Effect of feed rate on torque

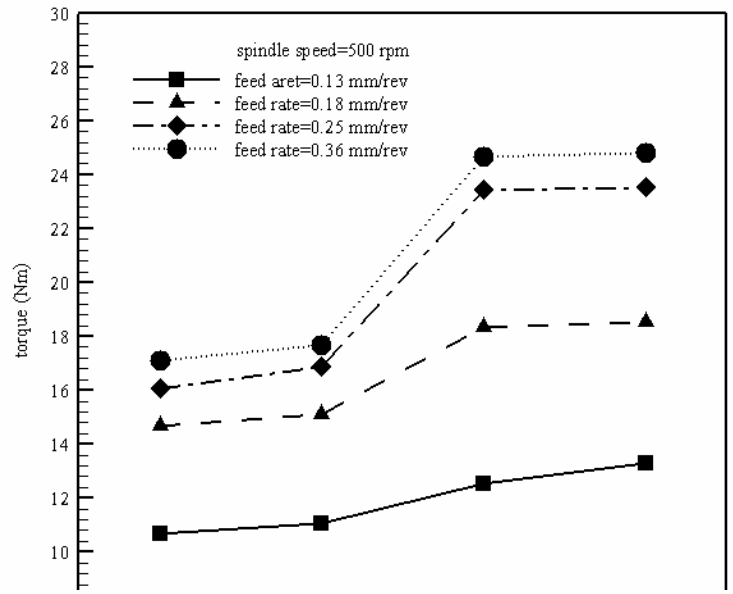

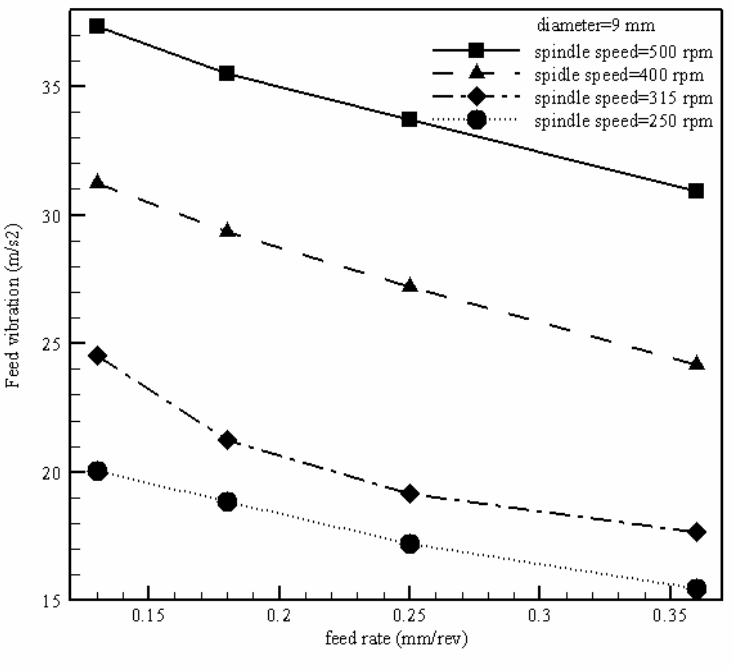

Fig. 8 Effect of drill diameter on torque

Fig. 9 Effect of feed rate on feed vibration

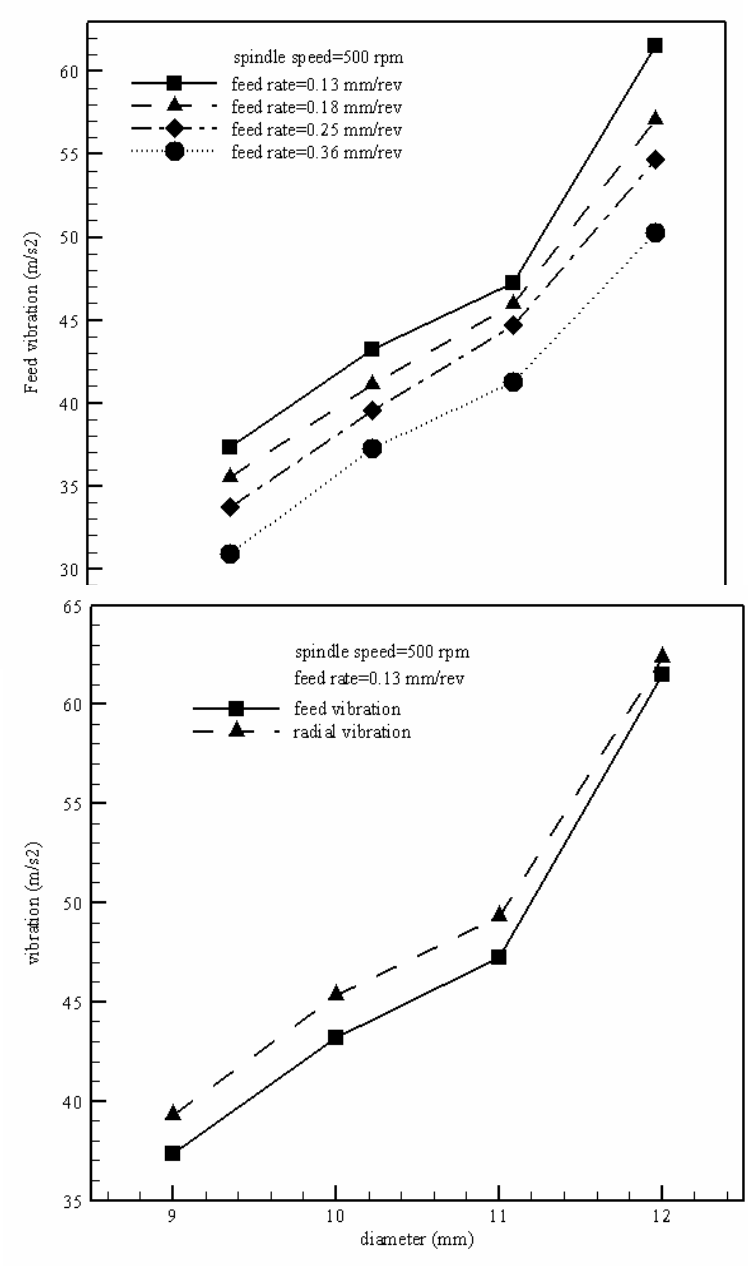

Fig. 10 Effect of drill diameter on feed vibration

Fig. 11 Variation of feed and radial vibration with drill diameter

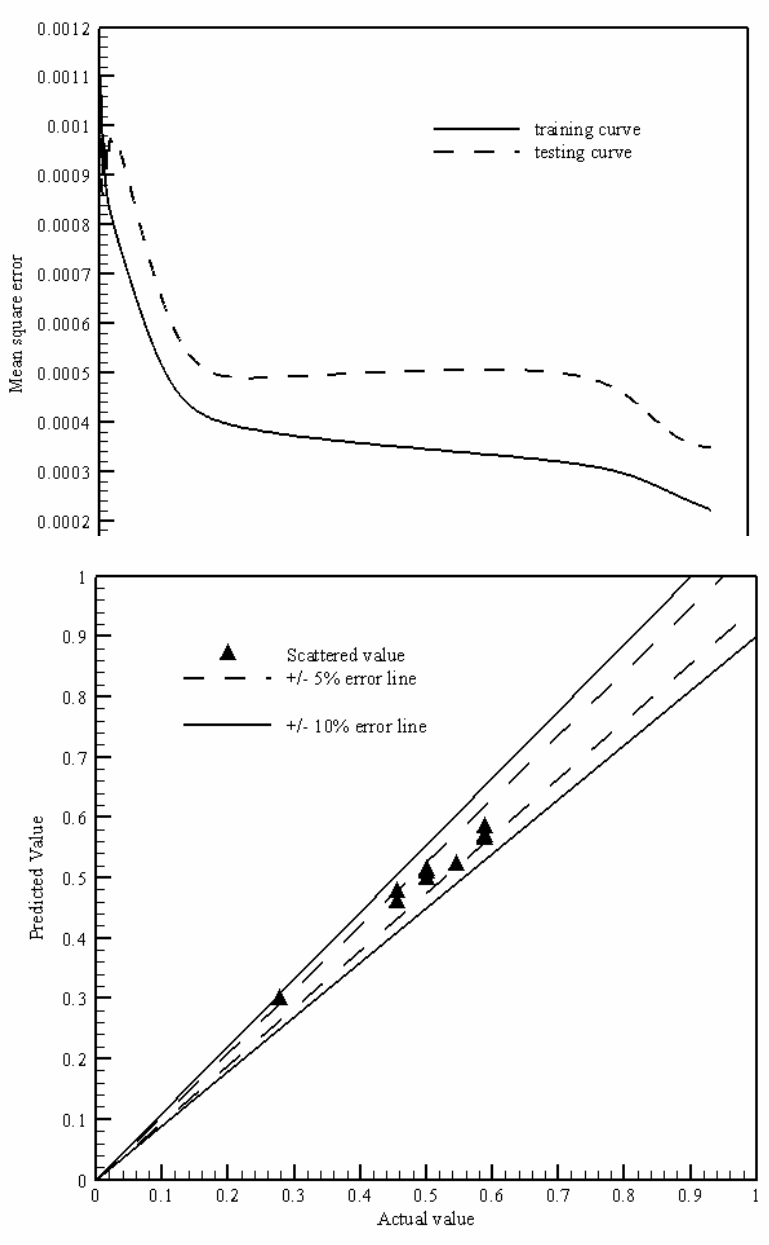

Fig. 12 Variation of mean square error with number of iteration for 5-7-1 architecture

with η =0.3 and α =0.9

Fig. 13 Comparison of Predicted value with actual value for 5-7-1 architecture with η =0.3 and α =0.9

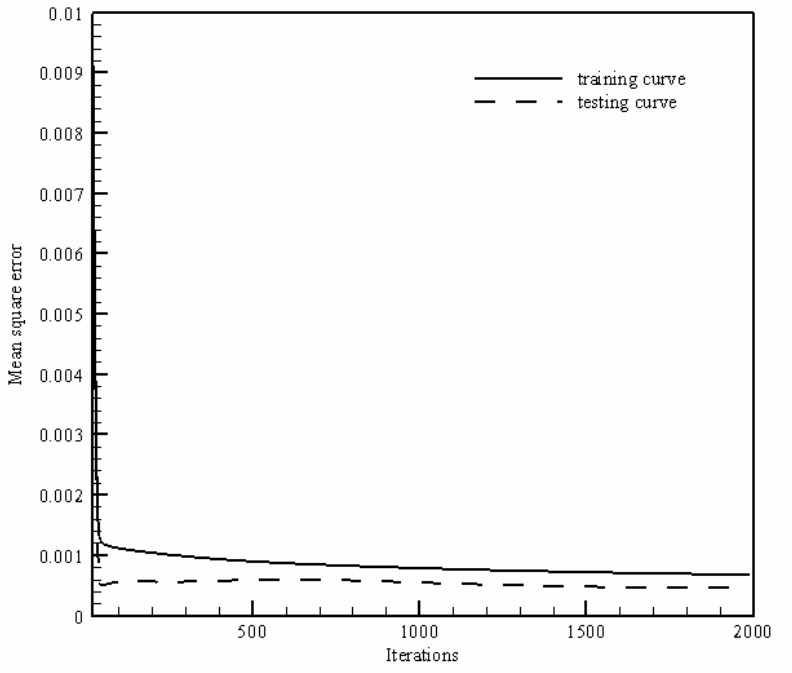

Fig. 14 Variation of mean square error with number of iteration for 6-3-1 architecture with η =0.3 and α =0.6

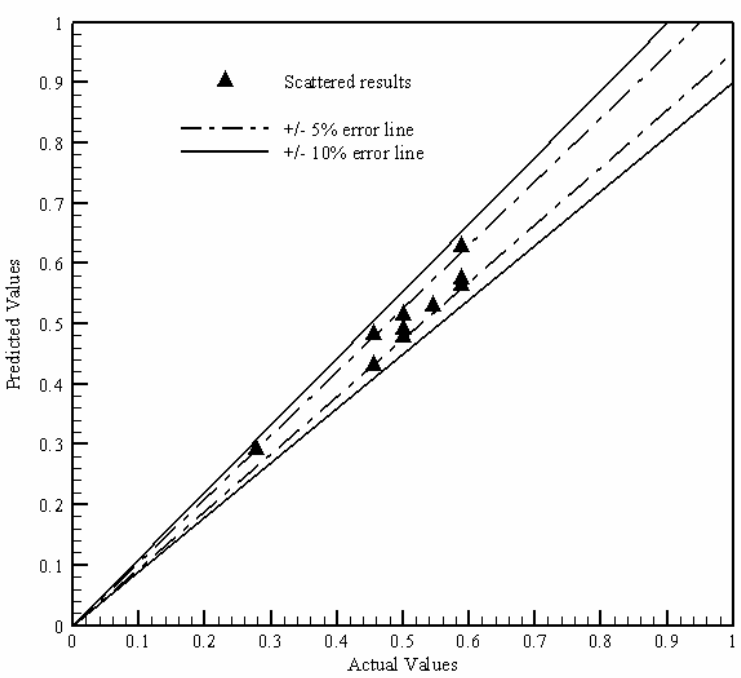

Fig. 15 Comparison of predicted values with actual values for 6-3-1 architecture with η =0.3 and α =0.6

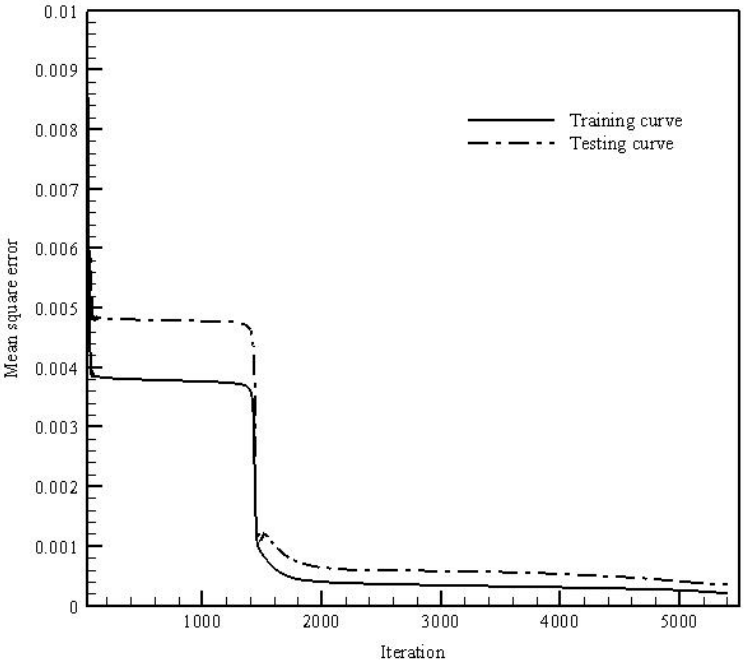

Fig. 16 Variation of mean square error with number of iteration for 7-10-1 architecture with η =0.6 and α =0.9

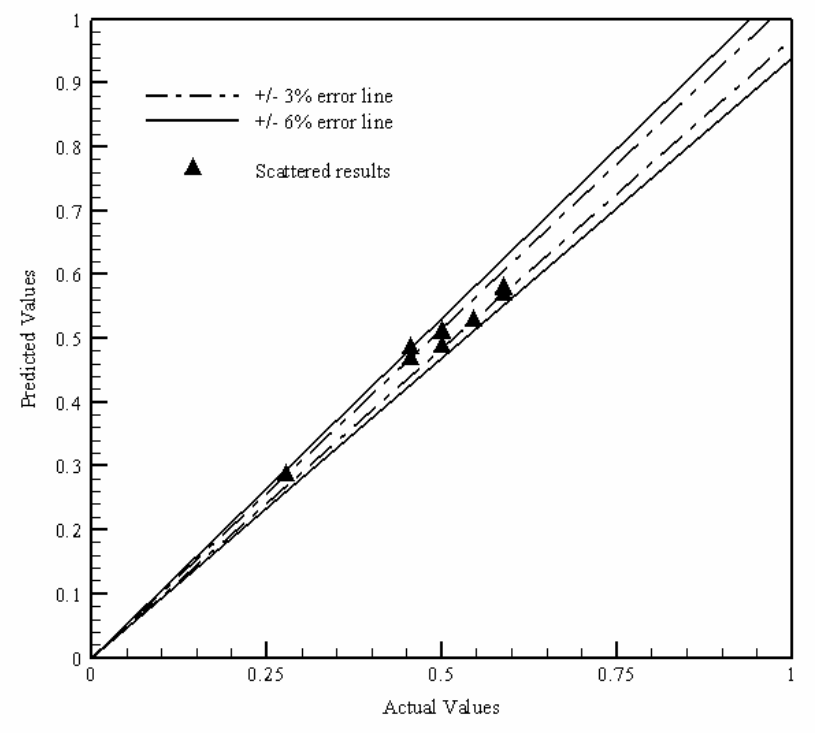

Fig. 17 Comparison of predicted value with actual value for 7-10-1 architecture with η =0.6 and α =0.9

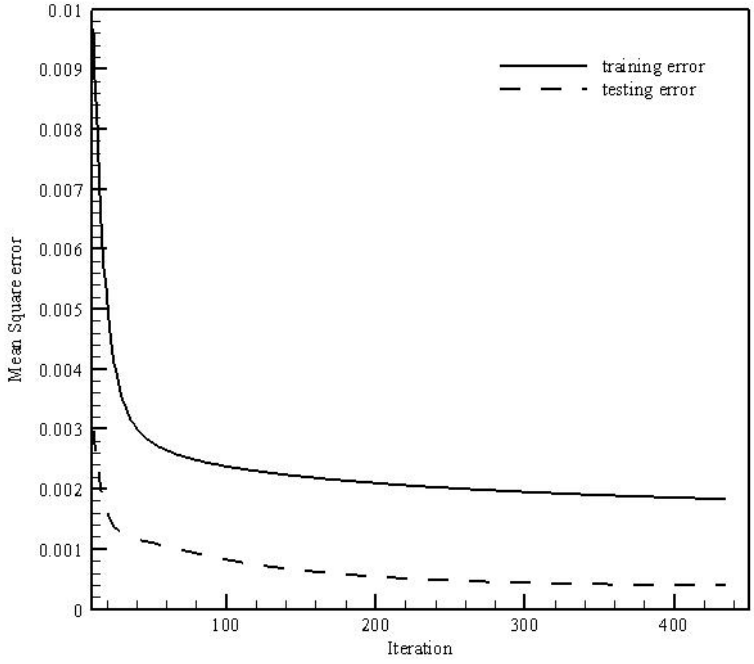

Fig. 18 Variation of mean square error with number of iteration for 7-40-1 architecture with $\eta = 0.3$ and $\alpha = 0.9$

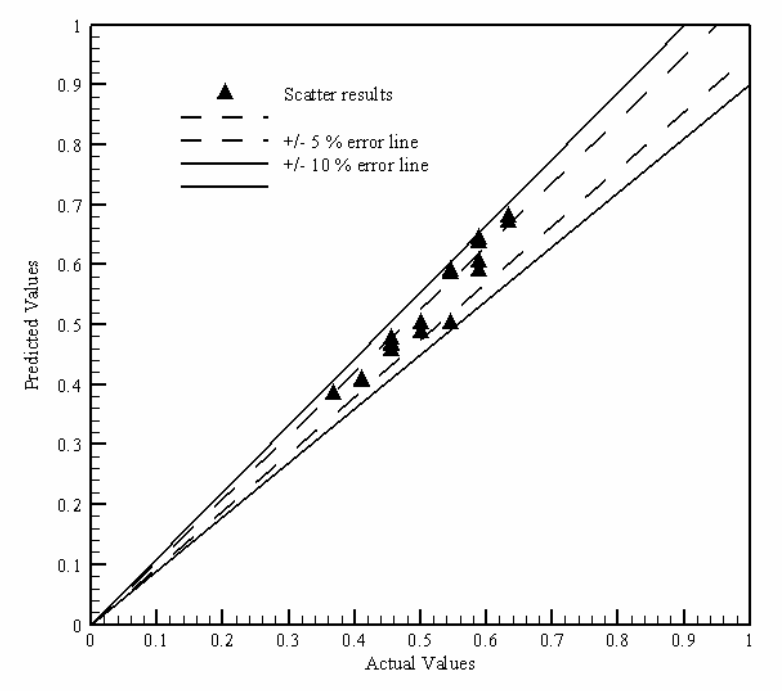

Fig. 19 Comparison of predicted value with actual value for 7-40-1 architecture with $\eta = 0.3$ and $\alpha = 0.9$

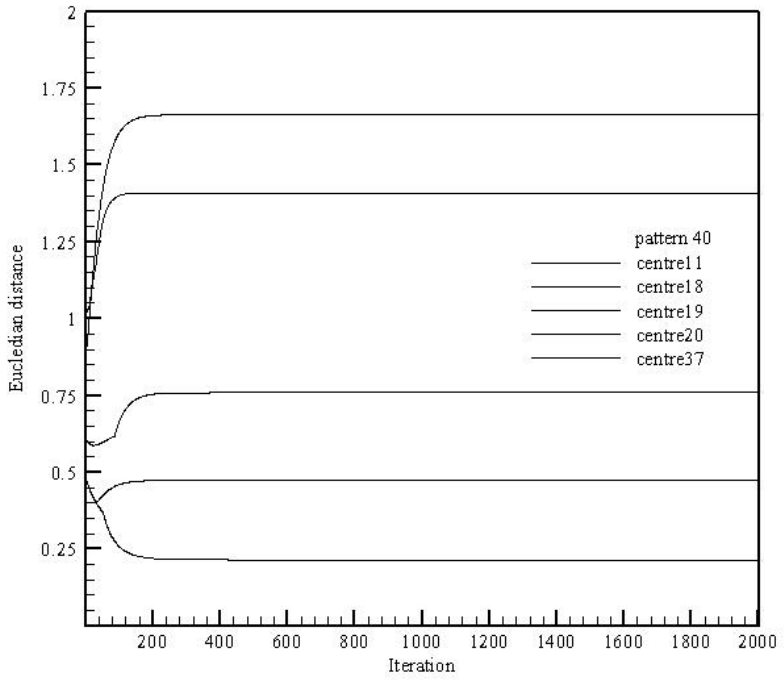

Fig. 20 Steady state condition of Euclidean distance for 7-40-1 architecture with $\eta = 0.3$ and $\alpha = 0.9$

Table 1 HSS drill geometry and chemical composition

(a) Geometry of HSS drill bit (long series)

Tool diameter (mm)	Flute length (mm)	Total length (mm)	Point angle(degree)	Helix angle(degree)
5	44.4	76.2	118	30
7.5	60.3	95.2	118	30
10	73	114.3	118	30

Flute	2 flutes
Flute type	parabolic
Shank type	straight cylindrical
Coating any	No

(b) Chemical Composition of HSS drill materials (wt%)

Tungston	Cromium	Vanadium	Cobalt	Molybdenum	Carbon	Hardness
18	4.3	1.1	5	0.65	0.75	290 BHN

Table 2 Cast iron properties and chemical composition

(a) Chemical composition

Fe	C	Si
94	3.5	2.5

(b) Mechanical properties

Ultimate tensile stress (MN/m^2)	Yield stress (MN/m^2)	Density (Kg/m^3)	Elongation (%)	Brinell Hardness
200-830	82-690	7000	5	262

Table 3 Experimental data of cast iron work-piece

Sl No	Diameter (mm)	Speed (rpm)	Feed (mm/rev)	Thrust Force (N)	Torque (Nm)	Feed vibration (m/s^2)	Radial vibration (m/s^2)	Flank wear (mm)
1	9	500	0.13	1088.1	10.67	37.36	39.28	0.1
2	9	500	0.18	1435.1	14.66	35.48	36.75	0.13
3	9	500	0.25	1588.3	16.04	33.72	35.52	0.06
4	9	500	0.36	1669.8	17.12	30.93	31.11	0.09
5	9	400	0.13	1150.9	11.22	31.24	33.22	0.12
6	9	400	0.18	1486.4	15.01	29.32	30.48	0.15
7	9	400	0.25	1642.8	16.36	27.21	27.86	0.1
8	9	400	0.36	1721.3	17.64	24.18	25.14	0.11
9	9	315	0.13	1185.2	11.43	24.52	25.12	0.15
10	9	315	0.18	1707.8	16.97	21.24	22.26	0.16
11	9	315	0.25	2025.8	20.06	19.14	21.32	0.11
12	9	315	0.36	2778	27.82	17.63	18.40	0.12
13	9	250	0.13	1212.4	11.47	20.06	21.16	0.16
14	9	250	0.18	1752.6	17.23	18.85	19.52	0.18
15	9	250	0.25	2077.1	20.35	17.21	18.10	0.13
16	9	250	0.36	2816.7	28.22	15.46	16.21	0.14
17	10	500	0.13	1188.3	11.06	43.21	45.30	0.07
18	10	500	0.18	1504.8	15.11	41.12	42.24	0.12
19	10	500	0.25	1668.9	16.85	39.54	40.44	0.11
20	10	500	0.36	1754.8	17.69	37.24	38.65	0.08
21	10	400	0.13	1215.6	11.18	39.54	41.26	0.08
22	10	400	0.18	1547.7	15.71	36.28	37.72	0.15
23	10	400	0.25	1715.2	17.08	35.44	36.42	0.14
24	10	400	0.36	1782.6	17.95	31.22	33.46	0.12
25	10	315	0.13	1627.3	15.8	33.27	35.52	0.11
26	10	315	0.18	1827.6	18.27	30.41	31.10	0.16
27	10	315	0.25	2786.7	27.84	28.26	29.67	0.16
28	10	315	0.36	3284.2	32.95	25.37	26.30	0.15
29	10	250	0.13	1677.3	16.01	27.30	28.69	0.12
30	10	250	0.18	1869.7	18.64	22.51	24.24	0.18
31	10	250	0.25	2824.2	28.11	20.52	22.60	0.17
32	10	250	0.36	3323.1	33.08	18.63	20.23	0.14
33	11	500	0.13	1254.9	12.54	47.26	49.32	0.1
34	11	500	0.18	1556.8	18.32	45.92	47.24	0.13
35	11	500	0.25	1724.3	23.41	44.66	45.54	0.14
36	11	500	0.36	1869.4	24.65	41.25	43.21	0.09
37	11	400	0.13	1318.6	13.04	43.22	44.62	0.11
38	11	400	0.18	2067	20.71	40.29	42.10	0.14
39	11	400	0.25	2538.9	25.42	38.23	39.28	0.15
40	11	400	0.36	2752.7	27.66	35.45	37.68	0.12
41	11	315	0.13	1342.9	13.61	36.03	37.41	0.13
42	11	315	0.18	2097	21.03	34.27	35.80	0.16

43	11	315	0.25	2753.8	27.68	31.58	33.41	0.16
44	11	315	0.36	2860.1	28.55	28.66	29.67	0.15
45	11	250	0.13	1394.6	13.88	31.24	33.14	0.17
46	11	250	0.18	2156.8	21.72	28.67	29.88	0.17
47	11	250	0.25	2885.6	28.04	27.49	28.62	0.18
48	11	250	0.36	3001.4	29.14	25.33	27.26	0.17
49	12	500	0.13	1277.8	13.28	61.51	62.36	0.14
50	12	500	0.18	1624.3	18.51	57.11	59.49	0.11
51	12	500	0.25	1856.3	23.51	54.62	56.24	0.1
52	12	500	0.36	2005.4	24.78	50.26	52.27	0.1
53	12	400	0.13	1464.3	14.39	56.58	58.12	0.16
54	12	400	0.18	2114.6	18.64	55.46	57.43	0.13
55	12	400	0.25	2558.6	23.58	51.12	53.22	0.17
56	12	400	0.36	2924.3	24.92	48.88	49.62	0.15
57	12	315	0.13	1524.6	15.28	48.26	49.24	0.17
58	12	315	0.18	2121.8	21.17	44.69	45.56	0.14
59	12	315	0.25	2612.6	26.21	41.52	43.37	0.21
60	12	315	0.36	3270	32.99	38.26	40.11	0.17
61	12	250	0.13	1578.2	15.62	41.72	43.76	0.2
62	12	250	0.18	2163.4	21.41	38.25	39.58	0.17
63	12	250	0.25	2672.6	26.52	35.68	37.20	0.24
64	12	250	0.36	3311.2	33.11	33.28	35.26	0.19

Table 4 Network Architecture for back propagation network

L=Number of neurons at input layer
M= Number of neurons at hidden layer
N=Number of neurons at output layer

η	α	**MSE training**	**MSE testing**	**Iteration**	**Max % error of validation**	**Mim % error of validation**	**Architecture L-M-N**	
.3	.2	0.000759	0.000458	3066	9.213052	-0.588035	5-5-1	**Without vibration**
.3	.5	0.000752	0.000455	2029	9.318743	-0.473577	5-5-1	
.3	.9	0.000492	0.00044	3200	11.321773	0.764639	5-5-1	
.8	.9	0.000104	0.000331	1709	-9.883300	0.007625	5-5-1	
.3	**.9**	**0.000221**	**0.000347**	**3495**	**-7.035090**	**-0.192109**	**5-7-1**	
.5	.9	0.000103	0.000335	6489	-7.388125	0.299454	5-7-1	
.8	.9	0.000057	0.000213	14254	-8.660548	-0.105009	5-7-1	
.3	.9	0.000267	0.000524	8478	-12.65958	-0.716748	5-10-1	
.3	.9	0.000282	0.000477	2431	9.098277	-0.279041	5-13-1	
.5	.8	0.000303	0.000807	7368	-11.07535	0.887593	5-13-1	
.3	.2	.000946	.000424	1143	-10.57	-0.88	5-3-1	
.3	.9	0.00054	0.000503	3762	9.54	-0.32	5-3-1	
.6	.6	0.003813	0.004748	318	15.65	0.38	5-1-1	
.1	.1	0.003817	0.004748	2124	15.66	0.48	5-1-1	
.1	.1	0.001202	0.000477	317	-8.42	0.19	6-3-1	**With feed vibration**
.1	.3	0.001204	0.000478	246	-9.86	-0.24	6-3-1	
.1	.9	0.000657	0.000481	1665	-11.95	-0.03	6-3-1	
.3	.1	0.000675	0.000446	4510	-6.84	-1.39	6-3-1	
.3	.3	0.0007	0.000456	2954	-7.75	1.37	6-3-1	
.3	**.6**	0.000673	0.000451	**1991**	**-6.25**	**2.16**	**6-3-1**	
.3	.9	0.000665	0.000493	718	-13.74	1.1	6-3-1	
.6	.3	0.000672	0.000446	1776	-11.6	-1.24	6-3-1	
.6	.6	0.000671	0.000456	997	12.99	-0.52	6-3-1	
.6	.9	0.000295	0.000402	3561	10.1	0.01	6-3-1	
.9	.1	0.000692	0.000435	1379	-11.11	0.25	6-3-1	
.9	.6	0.000668	0.00046	672	-7.66	1.18	6-3-1	
.1	.1	0.001164	0.000349	237	-8.02	-0.43	6-6-1	
.1	.9	0.000471	0.00047	6552	9.66	-0.2	6-6-1	
.3	.6	0.000082	0.00035	5631	-9.63	-0.45	6-6-1	
.6	.3	0.000504	0.000414	8066	9.25	0.53	6-6-1	
.6	.6	0.000482	0.000469	4094	8.61	-1.32	6-6-1	
.6	.9	0.000179	0.000344	3955	-7.46	-1.56	6-6-1	
.9	.1	0.00057	0.000444	6782	10.14	-0.61	6-6-1	
.9	.3	0.000543	0.000438	5417	9.77	1.06	6-6-1	
.9	.6	0.000491	0.000407	4051	11.05	-0.22	6-6-1	
.3	.2	0.000373	0.000404	21637	-10.09311	-1.032831	7-5-1	**With both vibration spectra**
.3	.5	0.000373	0.000402	13164	-10.04577	-1.059604	7-5-1	
.3	.9	0.000314	0.00044	2908	10.268342	0.366341	7-5-1	
.5	.5	0.000369	0.000395	8437	-10.03361	-1.239933	7-5-1	
.4	.6	0.00037	0.000394	8370	-9.998882	-1.182722	7-5-1	
.3	.3	0.000416	0.000315	7671	-10.10526	-0.874644	7-7-1	
.3	.5	0.000414	0.000315	5568	-10.14343	-0.826739	7-7-1	

.3	.9	0.000095	0.000281	6324	-9.673208	0.127836	7-7-1	
.4	.7	0.000417	0.000317	2485	-9.961436	-0.807868	7-7-1	
.3	.3	0.000676	0.000392	957	7.999867	0.552616	7-10-1	
.3	.9	0.000267	0.0004	4208	-7.165553	-0.488983	7-10-1	
.5	.9	0.000308	0.000442	1697	10.10424	-0.002049	7-10-1	
.2	.9	0.000367	0.000488	1381	9.454712	0.337459	7-13-1	
.5	.9	0.000253	0.000454	2142	9.751565	0.575089	7-13-1	
.6	**.9**	**0.000201**	**0.000356**	**5404**	**-6.177035**	**-1.259286**	**7-10-1**	
.8	.9	0.00028	0.000408	2623	10.339206	1.038324	7-5-1	
.7	.8	0.000031	0.000226	20097	16.473956	0.345249	7-5-1	
.1	.9	0.000379	0.000366	14299	10.938917	-0.376683	7-5-1	
.6	.9	0.000314	0.000299	351	-6.675638	-1.053119	7-8-1	
.7	.9	0.000082	0.000324	2061	-7.867673	0.518129	7-8-1	

Table 5 Network Architecture for SOM
L=Number of neurons at input layer
M= Number of centre vectors
N=Number of neurons at output layer

η	α	**MSE training**	**MSE testing**	**Iteration**	**Max % error**	**Mim % error**	**Architecture L-M-N**
.1	.6	0.003791	0.000439	4426	-16.51	0.07	7-20-1
.1	.9	0.001786	0.000486	1956	-15.68	-0.21	7-20-1
.3	.6	0.003791	0.000439	1478	-16.51	0.06	7-20-1
.3	.9	0.001786	0.000486	659	-15.68	-0.32	7-20-1
.6	.6	0.003789	0.000439	741	-16.50	0.05	7-20-1
.6	.9	0.001793	0.000487	289	-15.72	-0.47	7-20-1
.9	.6	0.003788	0.000439	495	-16.5	0.04	7-20-1
.1	.6	0.005128	0.000767	5509	15.89	0.45	7-30-1
.1	.9	0.003544	0.000843	102	-14.53	1.12	7-30-1
.3	.6	0.005122	0.000767	1843	15.89	-0.46	7-30-1
.6	.6	0.005112	0.000767	927	15.88	-0.49	7-30-1
.9	.6	0.005101	0.000767	622	15.87	-0.51	7-30-1
.1	.1	0.021258	0.006935	604	-41.61	-0.86	7-40-1
.1	.9	0.001812	0.000392	1374	-8.75	0.07	7-40-1
.3	**.9**	**0.001827**	**0.000393**	**435**	**8.20**	**-0.01**	**7-40-1**
.6	.9	0.001825	0.000393	220	-8.83	0.008	7-40-1